Measurement of resonant and nonresonant induced refractive index changes in Yb-doped fiber grating amplifier

Y. P. Shapira,* D. Oscar, B. Spektor, V. Smulakovsky, and M. Horowitz

Department of Electrical Engineering, Technion–Israel Institute of Technology, Haifa 32000, Israel
**Corresponding author: yuvalsh@tx.technion.ac.il.*

Received August 27, 2014; revised December 6, 2014; accepted December 23, 2014;
posted January 7, 2015 (Doc. ID 221421); published February 9, 2015

We have measured the refractive index change (RIC) induced in a fiber Bragg grating (FBG) written in a Yb-doped fiber amplifier (YB-FBG) because of the amplifier pumping. The measurement was performed by exploiting the high sensitivity of the YD-FBG transmission to the RIC. We have separated between electronic and thermal contributions to the RIC based on the difference between the time-scales of the two effects. Because of high UV-induced loss in FBGs, the thermal contribution to the RIC is increased, in comparison with previously published work, where no grating was written in the fiber amplifier. The measurement method allows us to find the sign of each contribution to the RIC, and it requires only a few centimeters of fiber. Optimal pumping scheme for reducing the RIC in a YB-FBG is studied.

OCIS codes: (050.2770) Gratings; (060.3735) Fiber Bragg gratings; (060.2320) Fiber optics amplifiers and oscillators.
http://dx.doi.org/10.1364/OL.40.000526

Optical fiber amplifiers have become essential components in optical communication systems [1], high-power optical applications [2,3], and optical sensors. Fiber Bragg gratings (FBGs) written in fiber amplifiers are widely used as distributed feedback (DFB) lasers [4,5] and DFB laser sensors [6]. Recently, we have shown theoretically that FBGs written in fiber amplifiers can be important for high-power optical pulse amplification [7]. In such a device, Kerr nonlinearity can help prevent pulse breaking as the amplified pulse peak power increases. Another advantage is the increase of the gain per fiber length because of reduction of the group velocity.

Pumping of fiber amplifiers results in refractive index change (RIC) in the fiber. In Refs. [8,9] the authors studied the RIC effects in Yb-doped fiber amplifiers (YDFA) by using an interferometric scheme. Two contributions to the RIC were found: a resonant electronic effect because of the polarizability difference between the excited and the ground state, and a resonant thermal effect. The resonant thermal effect addressed in Ref. [9] was caused by nonradiating atomic transitions. However, in FBGs, another significant source of thermally induced RIC exists: the writing of grating by UV illumination increases the absorption and loss over a broad frequency region [10]. This effect is referred to here as nonresonant thermal RIC.

In the case of a FBG written in a Yb-doped fiber amplifier (YD-FBG), the transfer function of the device is highly sensitive to the RIC along the grating. Hence, the operation of YD-FBGs strongly depends on the pumping in a complex way. Therefore, it is important to quantitatively study the RIC in such devices. The study is also important for DFB lasers that are based on fiber gratings [4,5] and for DFB laser sensors [6].

In this work we experimentally study the RIC in the YD-FBG. The measurement that is based on the high sensitivity of the transmission function of FBG to RIC, is simple and does not require interferometry. It requires only a short section of a YB-FBG with a length of about 10 cm. Hence, the effect of pump absorption on the results can be minimized. We could also measure the sign of the different RIC effects. The sign we measured was opposite to that obtained theoretically in a previous work [8,9], since in our experiments the pumping was significantly stronger than the pump saturation power. The separation between electronic and thermal RIC is based on the difference between the characteristic timescales of the two effects. Our results show that the RIC effect in YD-FBG is dominated by the nonresonant thermal effect associated with loss induced by writing of the FBG.

The experimental setup is described in Fig. 1. The YD-FBG was obtained in a Yb-doped fiber manufactured by CorActive (Yb118, fiber 3 in [8]). The small-signal absorption of Yb118 at a pump wavelength of 980.5 nm equals 147 dB/m. The transmission spectrum of the YD-FBG was

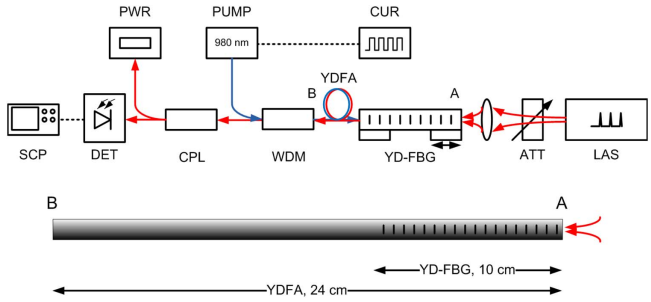

Fig. 1. Schematic drawing of the experimental setup and the YD-FBG fiber structure used in our experiments. LAS is a pulsed laser operating at 1064 nm (signal); ATT is a free-space optical attenuator; WDM is a wavelength-division-multiplexing coupler; PUMP is a continuous-wave (CW) pump laser source operating at 980.5 nm (pump); CUR is a pulsed current source used for driving PUMP laser; CPL is a directional coupler; PWR is a power meter; DET is an optical detector; and SCP is a real-time scope. The 10 cm long grating is written in a 24 cm long ytterbium doped fiber amplifier (YDFA). Side A of the YD-FBG is placed on a precise mechanical stage that allows stretching of the YD-FBG. Side B of the YDFA is spliced to the WDM coupler. The red color indicates the signal, while the blue color indicates the pump. The dotted lines indicate electrical signals.

measured by using a pulsed laser source (signal) at 1064 nm generating pulses with a repetition rate of up to 1 kHz, a width of 640 ps, and a peak power of 4 kW. The pulses were attenuated by a tunable attenuator and coupled into side A of the YD-FBG. Side A of the YD-FBG was held by a high-precision translation stage that could accurately stretch the grating, while side B was held by a fixed fiber holder. By moving the stage, the YD-FBG spectrum could be tuned with respect to the laser wavelength with a spectral resolution of 1.2 pm.

Side B of the YDFA was spliced to a 980/1064 nm wavelength division multiplexing (WDM) coupler to pump the YD-FBG in a back-pumping scheme. The splicing between the two different fiber types introduces loss that may cause heating. To reduce the influence of this effect on our measurements, the total amplifier length was increased to 24 cm, by adding a 14 cm long section of YDFA attached to side B of the YD-FBG. The pumping is performed by a CW laser source operating at a wavelength of 980.5 nm (pump). This laser is electrically pumped by using a pulsed current source with a controllable pulse width and amplitude. The output of the WDM coupler at 1060 nm is split by a directional coupler. One of the split signals was measured by using an optical power meter and the other by using an optical detector with a bandwidth of 5 GHz and a real-time oscilloscope. We note that, through the whole set of our experiments, the average power of the pulsed signal laser was three orders of magnitude lower than that of the pump. Hence the thermal effects associated with the signal could be neglected.

The FBG was a 10 cm-long grating with a 1.5 cm sine apodization section at both of its ends. The fiber was H_2 pre-loaded before the writing of the FBG to increase its photosensitivity [11]. The grating was written by using a scanning phase-mask technique [12]. While the phase-mask was scanned by a UV beam, the beam intensity was controlled to obtain apodization. By comparing the transmission bandwidth of the grating to the results of numerical simulations, we estimated the refractive index modulation amplitude of the grating as $\Delta n_1 = 2 \times 10^{-4}$. To coarsely tune the grating bandgap to the laser wavelength, the average refractive index along the grating was increased by removing the phase mask and scanning the fiber with a uniformly distributed UV beam. The obtained increase in average refractive index due to the grating was $\Delta n_0 = 2.1 \times 10^{-3}$. Hence, in our experiments $\Delta n_0 \gg \Delta n_1$. The maximum grating transmission was $\max(T) = 0.77$, corresponding to grating UV-induced loss of −11.5 dB/m. The measured loss is similar to the UV-induced loss that can be estimated according to Ref. [10] for a grating strength of $\Delta n_1 = 2.1 \times 10^{-3}$.

Figure 2 shows the normalized grating transmission spectrum $T_n = T/\max(T)$. The transmission is presented at different resolutions. Figure 2(c) shows that the grating transmission spectrum monotonically changes as a function of the wavelength by more than 30 dB at the red side of the transmission band. This spectrum region is used in our experiments to measure the RIC. The experiments described below were conducted at two operating points indicated on the transmission spectrum in Fig. 2 by vertical lines: λ_1, characterized by a normalized transmission (in the absence of pumping) $T_n = 100\%$,

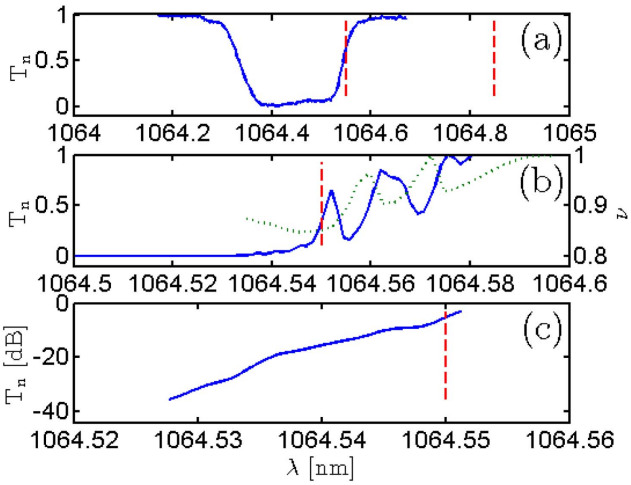

Fig. 2. Transmission spectrum of an unpumped YD-FBG: (a) low resolution wide-band spectrum measured by using amplified spontaneous emission (ASE) source and a spectrum analyzer with a resolution of 10 pm; (b),(c) high resolution spectrum measurement of the long-wavelength side of the grating transmission spectrum, with a spectral resolution of 1.2 pm. The measurement was obtained by a controllable stretching of the fiber and monitoring the power of the transmitted signal by an optical power meter. The red dashed vertical lines indicate the two operating points used in our experiments: λ_1, where the normalized transmission of the (unpumped) YD-FBG equals $T_n = 100\%$, and λ_2, where the normalized transmission equals $T_n = 30\%$. The green dashed–dotted line in (b) shows the measured pulse group velocity $\nu \times Vg$ as a function of the wavelength, where Vg is the group velocity in the fiber.

and λ_2, characterized by a normalized transmission of $T_n = 30\%$. The operating point λ_1 is located far from the bandgap, and therefore is not sensitive to the small RIC. The operating point λ_2, on the other hand, is located in close vicinity to the grating bandgap and hence is highly sensitive to the RIC.

Figure 3 shows the measured dependence of the signal transmission on the duty cycle (DC) of the pump pulses in a steady state condition. The pump and signal pulse repetition rate equals 50 Hz. For the operating point

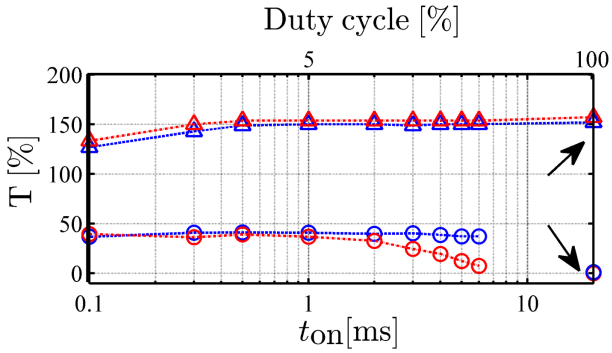

Fig. 3. Transmission of the signal through pumped YD-FBG at a steady state as a function of the pump pulse width, t_{on}. The pulse repetition rate equals 50 Hz. The circles correspond to operating point λ_2, and the triangles correspond to λ_1. The blue dashed line corresponds to a pump peak power of 15.6 dBm and the red dashed–dotted line corresponds to a pump peak power of 17.9 dBm.

λ_1, the transmission increases as the DC of the pump pulses increases because of increase in the gain. The signal gain for a continuous wave (CW) pumping increases by 3.5% when the pump power is increased by the factor of 1.7, indicating that the fiber amplifier is saturated. As the pump DC increases, the average pump power increases and hence the thermally induced RIC also increases. As a result, the grating spectrum is shifted toward longer wavelengths. While the signal at λ_1 is almost unaffected by the spectral shift, the transmission of the signal operating at λ_2 shows a complex behavior. In this case, the transmission is affected by the interplay between two dominant effects: the increase in transmission because of increased gain, and the decrease in transmission because of increased thermally induced RIC. Hence, for pulse widths shorter than about 1 ms, the transmission remains almost constant when the DC increases, as the two effects nearly cancel each other. For pulse widths longer than about 1 ms, the average pump power is further increased, the thermal effect becomes dominant, and the transmission is dramatically reduced. Therefore, to obtain maximum transmission, the optimal pump pulse width should be between 1 and 2 ms, depending on the pump power.

To separate the electronic and thermal RIC effects, we have measured the transient transmission of the signal after the pump is turned off. The two operating conditions marked in Fig. 3 by arrows, that correspond to a CW pumping, were the starting points for these measurements. To obtain high temporal resolution, the signal pulse repetition rate was increased to 1 kHz, while the signal peak power was decreased by the factor of 20, keeping the average signal power unaffected. The results are shown in Fig. 4.

Figure 4 shows the transmission evolution of the signal at λ_1. Since this operating point is located far from the grating bandgap, the transmission is not sensitive to the small RIC. Therefore, after switching off the pump, the normalized transmission gradually decreased from $A_1 = 152\%$ to $C_1 = 100\%$ and reached its steady-state

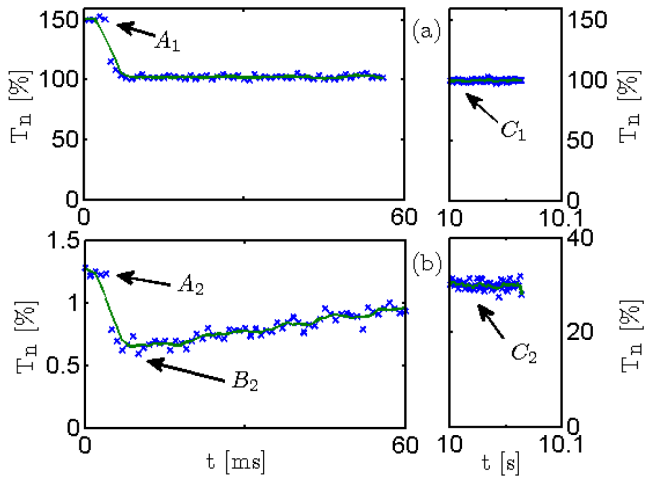

Fig. 4. Dynamics of the YD-FBG transmission for operating points (a) $\lambda = \lambda_1$ and (b) $\lambda = \lambda_2$ after the pump is switched off at time marked by arrows located at the vicinity of the notations A_1 and A_2. Before the pump was switched off, the amplifier was CW pumped with a power of 15.6 dBm.

value after about 2 ms. From the transmission at points A_1 and C_1, shown in Fig. 4, we can calculate the signal gain added by the YDFA: $\Delta g = A_1/C_1 = 1.52$. Figure 4 shows the signal transmission evolution at λ_2. The transmission dynamics in this case are affected by three effects: (i) change in the optical gain; (ii) electronic RIC; and (iii) thermal RIC. At a steady state, before the pump was switched off, the normalized transmission was $A_2 = 1.25\%$. The timescale of the electronic effects in YDFA is on the order of $\tau_{\mathrm{el}} = 1$ ms [2]. Within the first few milliseconds after the pump switch-off, the transmission of the grating decreases. This timescale corresponds to τ_{el} and therefore the transmission decrease is caused by the combination of effects (i) and (ii). After few ms the transmission starts to gradually increase, toward its steady-state value without pumping, $C_2 = 30\%$, with a characteristic time of about 5 sec, which is associated with the thermal RIC.

To estimate the magnitude of the two different RIC effects, we make the simplifying assumption that the RIC is uniform along the grating length. In our experiments, the pump power decreases by about 50% along the YD-FBG and hence the RIC is not uniformly distributed. However, by using a numerical simulation, we obtained that the analysis described below gives the average RIC along the YD-FBG with an error of only few percent.

From the measured transmission of the three marked points at Fig. 4: A_2, B_2, and C_2, we obtain $T^{\lambda_2}_{i,ii,iii} = A_2$ and $T^{\lambda_2}_{iii} = B_2$, where $T^{\lambda_2}_{i,ii,iii}$ is the grating normalized transmission at λ_2, resulting from the combination of effects (i), (ii), (iii); and $T^{\lambda_2}_{iii} = 0.65\%$ is the normalized transmission resulting from the thermal RIC. We note that the gain change Δg is obtained because of the turnoff of the pumping along the whole 24 cm section of the YDFA while the change in the transmission T is obtained only in the YD-FBG.

In general, the optical gain changes because of the RIC since the small signal gain depends on the group velocity [13]. Figure 2(b) shows the measured group velocity, $\nu \times V_{\mathrm{g}}$, where V_{g} is the fiber group velocity without the grating. The measurement was performed by a direct measurement of the pulse propagation time along the grating as a function of the wavelength, by using a real-time oscilloscope. The minimal group velocity measured in a wavelength region of ± 20 pm around λ_2 equals $\nu = 0.85$. As a result, the gain Δg is expected to change by up to 3% because of the RIC [13]. We also verified by using a numerical simulation that the small gain changes do not significantly affect the profile of the grating transmission spectrum. Hence we obtain $A_2 = \Delta g \times T^{\lambda_2}_{ii,iii}$, where $T^{\lambda_2}_{ii,iii} = 0.83\%$ is the normalized grating transmission caused by the combination of effects (ii) and (iii). We next use the transmission spectrum shown in Fig. 2(c) to calculate the corresponding wavelength change $\Delta\lambda$ and the RIC, and obtain electronic RIC equals $\Delta n_{ii} = -0.7 \times 10^{-6}$, and thermal RIC equals $\Delta n_{\mathrm{iii}} = 2.1 \times 10^{-5}$.

The obtained electronic RIC can be compared to the results obtained for the same type of fiber (fiber 3) in Ref. [8]. For the input pump power of 15.6 dBm, the absolute value of the average electronic RIC obtained in [8] equals $\langle \Delta n_{ii} \rangle = |\int n_{ii}(z)\mathrm{d}z/L| = 0.79 \times 10^{-6}$, where

$L = 2$ m is the amplifier length. Hence, the electronic RIC we obtained is in accordance with the average electronic RIC as obtained in [8]. However, in [8] the electronic RIC was proportional to the pump input power. This dependence can be explained by the high depletion of the pump in that experiment since the fiber length was long. In our experiments, we could use YDFA with a length that is an order of magnitude shorter than in [8]. Therefore, the pump depletion is small and the amplifier is saturated along its whole length as shown in Fig. 3.

The magnitude and the sign of the electronic RIC depend on the pump wavelength and its power. In our experiments, the pump power was almost two orders of magnitude higher than the pump saturation power, and its wavelength was 980.5 nm. Since at that wavelength the absorption and the emission cross sections are nearly equal, about 50% of the Yb ions occupy the excited energy state [2]. We have calculated the theoretical electronic RIC based on emission and absorption spectra provided by the fiber manufacturer, by using the Kramers–Kronig relations. The calculation was performed for different values of excited-state ion population. The results show that, for an exited state population higher than 40%, the electronic RIC is negative, as obtained in our measurements. For lower pump power, the electronic RIC becomes positive, as in [9]. Because of the pronounced four-level behavior of YDFA at 1064 nm [2], the low energy state is nearly unpopulated and it is possible to obtain a significant gain with zero electronic RIC.

In our experiments, the thermal RIC is significantly stronger than the electronic RIC. This result is in agreement with [9]. However, the obtained value of the thermal RIC in [9] is three times smaller than was obtained in our experiments. This difference is explained by the excess wide-band loss induced during the writing of the grating. Hence, the dominant RIC effect in the YD-FBG is the nonresonant thermal effect [10].

In conclusion, we have studied the refractive index change (RIC) induced in fiber Bragg gratings (FBG) written in a Ytterbium-doped fiber amplifier (YD-FBG) as a result of optical pumping. The RIC has two contributions: electronic effect, due to polarizability difference between the excited and the ground electronic states, and thermal effect, due to non-radiative electronic transitions and due to loss induced during the writing of the grating. We have measured the timescales and the magnitudes of both effects. When the amplifier is in deep saturation, the electronic RIC is negative. The timescale of the thermal RIC is 3 orders of magnitude longer than that of the resonant RIC, and its magnitude is 30 times higher. The pumping of a YD-FBG can be optimized by modulating the pump and controlling the pump pulse width and amplitude. The measurement of the RIC in fiber amplifiers by using a YD-FBG is a sensitive measurement that requires only a few centimeters of fiber. The dependence of the RIC on the pumping is important for distributed feedback fiber lasers, as well as for fiber laser sensors.

This work was supported by the Israel Science Foundation (ISF) of the Israel Academy of Sciences (grant no. 1092/10).

References

1. E. deSurvire, IEEE J. Lightwave Technol. **8**, 1517 (1990).
2. R. Paschotta, J. Nilsson, A. C. Tropper, and D. C. Hanna, IEEE J. Quantum Electron. **33**, 1049 (1997).
3. D. J. Richardson, J. Nilsson, and W. A. Clarkson, J. Opt. Soc. Am. **B27**, B63 (2010).
4. J. T. Kringlebotn, J. L. Archambault, L. Reekie, and D. N. Payne, Opt. Lett. **19**, 2101 (1994).
5. A. Asseh, H. Storoy, J. T. Kringlebotn, W. Margulis, B. Sahlgren, S. Sandgren, R. Stubbe, and G. Edwall, Electron. Lett. **31**, 969 (1995).
6. D. J. Hill, B. Hodder, J. De Freitas, S. D. Thomas, and L. Hickey, Proc. SPIE **5855**, 904 (2005).
7. Y. P. Shapira and M. Horowitz, Opt. Lett. **37**, 3024 (2012).
8. A. A. Fotiadi, O. L. Antipov, and P. Mégret, Opt. Express **16**, 12658 (2008).
9. M. S. Kuznetsov, O. L. Antipov, A. A. Fotiadi, and P. Mégret, Opt. Express **21**, 22374 (2013).
10. I. C. M. Littler, T. Grujic, and B. J. Eggleton, Appl. Opt. **19**, 4679 (2006).
11. P. J. Lemaire, R. M. Atkins, V. Mizrahi, and W. A. Reed, Electron. Lett. **29**, 1191 (1993).
12. K. O. Hill, B. Malo, F. Bilodeam, D. C. Johnson, and J. Albert, Appl. Phys. Lett. **62**, 1035 (1993).
13. Y. P. Shapira and M. Horowitz, Opt. Lett. **34**, 3113 (2009).